



Analysis of the Effect of Gothic Vortex Generator Using Computational Fluid Dynamic on Naca 2412

Zidhane Aliffaputra Nuranto^(✉), Setyo Hariyadi Suranto Putro,
and Nyaris Pambudiyatno

Politeknik Penerbangan Surabaya, Jemur Andayani I/73, Wonocolo Surabaya 60236,
Jawa Timur, Indonesia
zidhane290301@gmail.com

Abstract. A vortex generator is a small component that has shaped as a fin and located on upper the surface of the wing or stabilizer to do modification the air-flow around the wing surface that affects the boundary layer. In this research, analysis of the aerodynamic characteristic has been done by using computational fluid dynamics (CFD). The purpose of this analysis is to find out the difference in the airflow between NACA 2412 with an additional gothic vortex generator and NACA 2412 without an additional vortex generator, and also to find out the airflow characteristic on NACA 2412 with varying angle of attack. The Research method used is analysis simulation on test object airfoil NACA 2412 with an additional gothic vortex generator with straight configuration with the angle of attack variation 0° , 2° , 4° , 6° , 8° , 10° , 12° , 15° , 16° , 17° , 19° , 20° , 23° , and 25° . Space between installed vortex generator is 60 mm with the size of vortex generator length is 25 mm, height 10 mm, and installed on $x/c = 10\%$ and 15% direct to chord line from the leading edge. The result of the research shows that the additional vortex generator on NACA 2412 can delay airflow separation. In 15% additional position direct to the chord line from the leading edge has better distribution and the highest lift coefficient, so in this research, the 15% additional position direct to the chord line from the leading edge is the most effective to use.

Keywords: Vortex Generator · Airfoil · Aerodynamic · NACA 2412

1 Introduction

A Vortex generator (VG) is a small component that has a fin shape and is usually located on the wing surface or stabilizer to affect the boundary layer. The additional of vortex generator could delay the air separation so the performance of the wing increase. The research of vortex generators is a form of development in aerodynamics. There are a lot of ways to analyze the performance of aerodynamics and one of them is using a wind tunnel. The Wind tunnel is an instrument that is used to research the aerodynamic effect

when the air is passing through a solid object. But, as time progresses the technology has grown fast, and the analysis process can be done even at home using computational fluid dynamic (CFD). Computational Fluid Dynamics (CFD) is one of the methods that can be used to research aerodynamics. CFD is filled with a set of methodologies using a computer that can be used to simulate fluid flow, heat transfer, chemical reaction, etc. The working principle of CFD is the object experiment will be divided into a cell and will be processed called meshing. CFD can be accessed using computer software. Some of the software are ANSYS, Exceed, CATIA, etc. This research is intended to know the effect of an additional gothic vortex generator on the upper wing surface of NACA 2412. Research on vortex generators has been carried out by many experts including López Calle [1], Boonloi et al. [2], Velte et al. [3], Shim et al.[4] etc. However, this topic is interesting to dig deeper so that almost every year there are always new developments regarding vortex generators.

2 Method

2.1 Boundary Condition

A boundary condition is a condition where the control of calculation is defined as an early definition and becomes the boundary of flow that passes through the object by determining the walls, inlet, and outlet. Boundary conditions should be by the shape of the object (Fig. 1).

2.2 Meshing

The Meshing process is a process to divide volume from the geometry object into small parts so the calculation results are more accurate. According to Anderson [7] and Kontogiannis [8] criterion, the next research stage will use mesh B (Table 1).

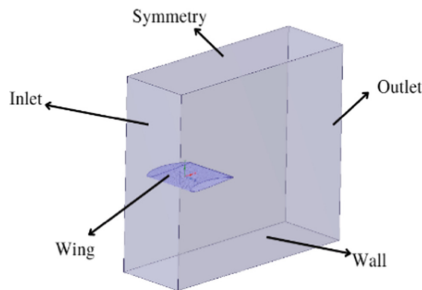


Fig. 1. Domain and Boundary Condition [5, 6]

Table 1. Mesh grid independency

Meshing	Node	Elements	C _D
Meshing A	429505	2283546	0,12065
Meshing B	537020	3089741	0,2308
Meshing C	647850	3598976	0,24821
Meshing D	758655	4132478	0,29078
Meshing E	864350	4802637	0,30063

3 Numeric Simulation Result

Designing the geometry model using Solidworks 2019 software and analysis, the aerodynamics using ANSYS Fluent using 20 m/s velocities and air density of 1.225 kg/m³. The result from the simulation is flow visualization when the air passes through the airfoil and also the lift coefficient and drag coefficient.

3.1 Drag Coefficient

From Fig. 2, it is shown that the drag coefficient to $\alpha = 0^\circ, 2^\circ, 4^\circ, 6^\circ, 8^\circ, 10^\circ, 12^\circ, 15^\circ, 16^\circ, 17^\circ, 19^\circ, 20^\circ, 23^\circ, 25^\circ$. From this figure, the aerodynamic performance of NACA 2412 with an additional vortex generator and without a vortex generator can be seen. The drag coefficient provided by NACA 2412 without a vortex generator has a higher amount than the NACA 2412 with an additional vortex generator. On NACA 2412 without a vortex generator, the drag coefficient increases to a maximum on $\alpha = 12^\circ$ with the amount 0,45702 and begin to decrease on the angle of attack $\alpha = 15^\circ$. On NACA 2412 with an additional vortex generator, the drag coefficient increase to a maximum on the angle of attack $\alpha = 17^\circ$ with the amount 0,51917 at 10% installation position direct to chord line and 0,491891 at 15% installation position direct to chord line.

3.2 Lift Coefficient

Figure 3 shows that the lift coefficient to $\alpha = 0^\circ, 2^\circ, 4^\circ, 6^\circ, 8^\circ, 10^\circ, 12^\circ, 15^\circ, 16^\circ, 17^\circ, 19^\circ, 20^\circ, 23^\circ$, and 25° . From this figure, the aerodynamic performance of NACA 2412 with an additional vortex generator and without a vortex generator can be seen. The lift coefficient provided by NACA 2412 without a vortex generator has a lower amount than the NACA 2412 with an additional vortex generator. On NACA 2412 without a vortex generator, the coefficient lift increases to a maximum on the angle of attack $\alpha = 12^\circ$ with the amount 3,195271 and begin to decrease on the the angle of attack $\alpha = 15^\circ$. On NACA 2412 with an additional vortex generator, the coefficient lift increases to a maximum on the angle of attack $\alpha = 17^\circ$ with the amount 3,49720 at 10% installation position direct to chord line and 3,621980 at 15% installation position direct to chord line.

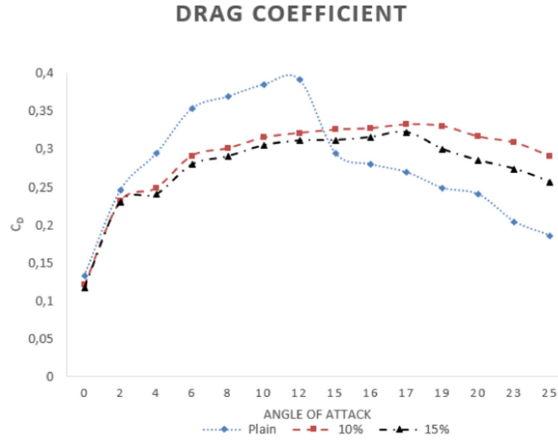


Fig. 2. Drag Coefficient

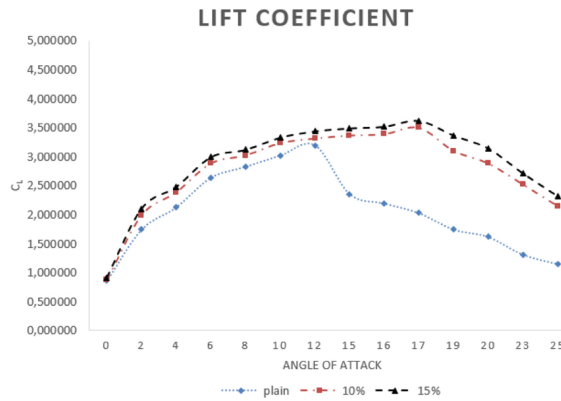


Fig. 3. Lift Coefficient

3.3 Lift-To-Drag Ratio (C_L/C_D)

From lift coefficient and drag coefficient, it can determine the lift-to-drag ratio (C_L/C_D) as shown in Fig. 4. These are the figure of the lift-to-drag ratio to $\alpha = 0^\circ, 2^\circ, 4^\circ, 6^\circ, 8^\circ, 10^\circ, 12^\circ, 15^\circ, 16^\circ, 17^\circ, 19^\circ, 20^\circ, 23^\circ$, and 25° . From this figure, the aerodynamic performance of NACA 2412 with an additional vortex generator and without a vortex generator can be seen.

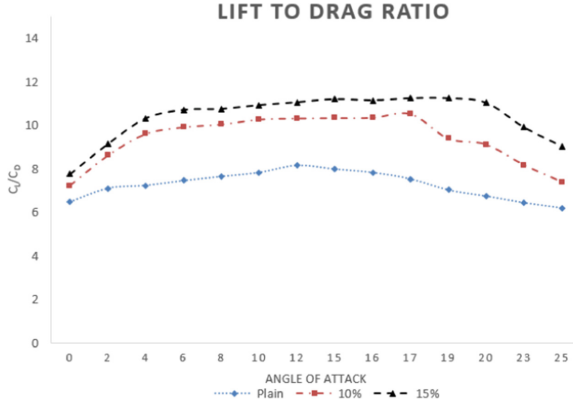


Fig. 4. Lift-to-drag Ratio

From the figure above can be seen that if the angle of attack increases so the lift-to-drag ratio amount is also increasing. On NACA 2412 without a vortex generator, the lift-to-drag increases to a maximum on $\alpha = 12^\circ$ with the amount 8,167 and begin to decrease on the angle of attack $\alpha = 15^\circ$. On NACA 2412 with an additional vortex generator, the drag coefficient increases to a maximum on the angle of attack $\alpha = 17^\circ$ with the amount 10,536 at 10% installation position direct to chord line and 11,252 at 15% installation position direct to chord line.

3.4 Velocity Magnitude Contour

This part will be shown how is the visualization from the simulation result on NACA 2412 with an additional vortex generator and NACA 2412 without a vortex generator with the purpose to complete the explanation from the simulation that has been done. Figure 5 is the figure of velocity contour from NACA 2412 at the angle of attack 0° , from Fig. 5 the significant difference has not been shown yet because the three airfoils are still in normal condition so the flow separation has not been shown yet. Figure 6 is the figure of velocity contour from NACA 2412 at $\alpha = 17^\circ$, from Fig. 6 can be seen there are differences between colors provided by the wing with an additional gothic vortex generator and the wing without a vortex generator. The wing without a vortex generator has an area colored with blue more dominant than the wing with an additional vortex generator on the wing's upper surface and that is describing there is a boundary layer that generates bigger flow separation. So we can conclude that the vortex generator can delay the flow separation so the wing performance of the wing is increased and the lift can be maintained as shown in figures (b) and (c) in Fig. 6. Figure 7 is the figure of velocity contour from NACA 2412 at $\alpha = 25^\circ$, from Fig. 7 can be seen on all of the wings has larger flow separation and causing all of the wings to lose their lift. So can be concluded that if the angle of attack increases larger flow separation can happen.

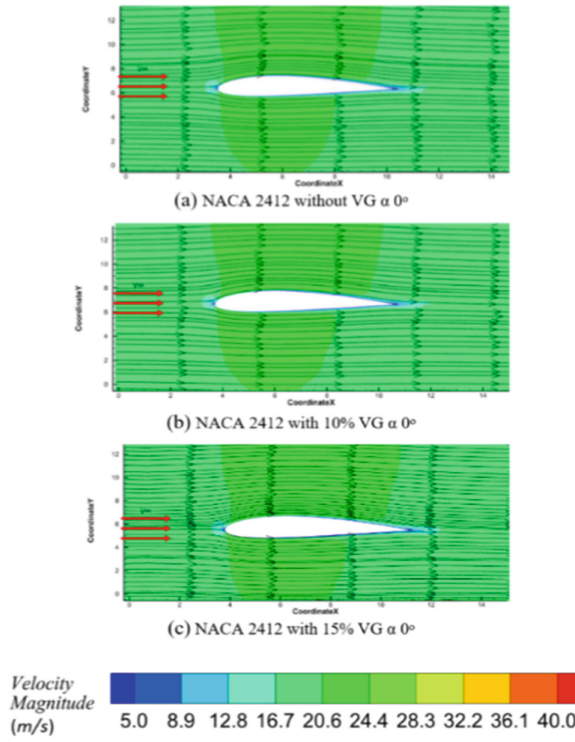


Fig. 5. Velocity contour $\alpha = 0^\circ$. (a) NACA 2412 without VG (b) NACA 2412 with 10% VG (c) NACA 2412 with 15% VG

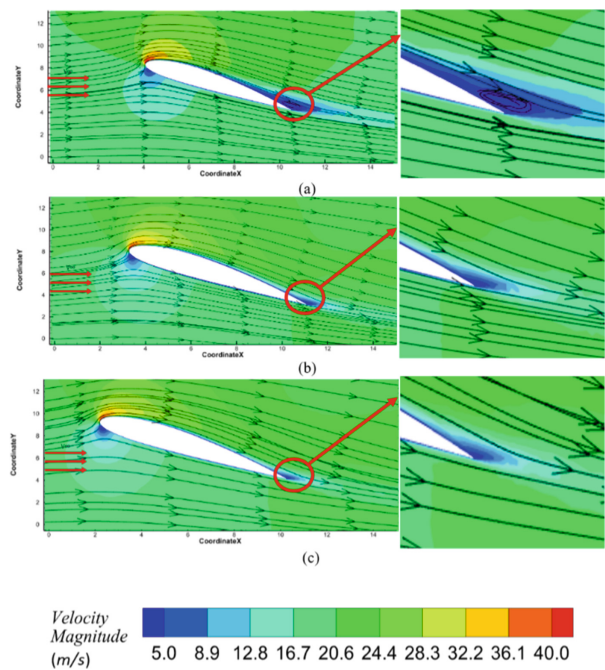


Fig. 6. Velocity contour $\alpha = 17^\circ$. (a) NACA 2412 without VG (b) NACA 2412 with 10% VG (c) NACA 2412 with 15% VG

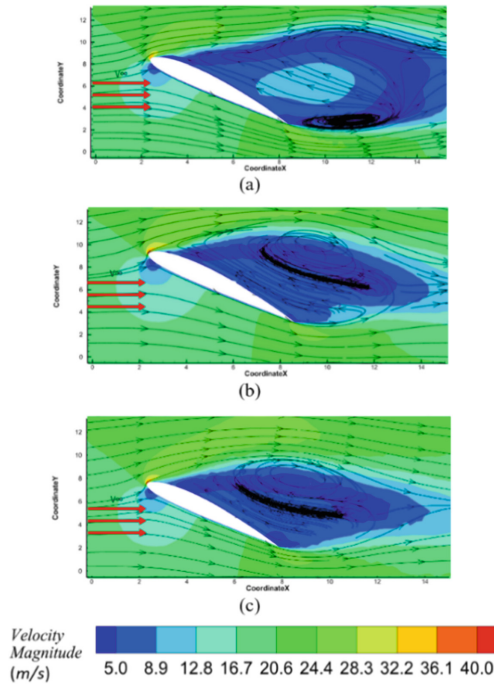


Fig. 7. Velocity Contour $\alpha = 25^\circ$. (a) NACA 2412 without VG (b) NACA 2412 with 10% VG (c) NACA 2412 with 15% VG

3.5 Vorticity Magnitude Contour

Vorticity magnitude is an area where things has tends to turn and have shape deformation. This vorticity magnitude contour is a result of the simulation on NACA 2412 at $\alpha = 0^\circ, 17^\circ$, and 25° in the area near the wing tip. From Figs. 8, 9, and 10 can be seen that at $\alpha = 0^\circ$ area colored red has more narrow than at $\alpha = 17^\circ$ and 25° . In Fig. 9, it can be seen at the plain airfoil has an area colored red more full than the airfoil with an additional vortex generator. On the airfoil with an additional vortex generator, there is an area colored red shorter than the plain airfoil, so it can be concluded that on a plain airfoil the tendency of air to turn is bigger than the airfoil with an additional vortex generator. In Fig. 10, it can be seen there is an area colored red on all airfoils has a larger area than in Figs. 8 and 9. The condition on all wings in Fig. 10 is wing has stalled (losing lift force) so the tendency of air to turn is larger, and can be concluded that if the angle of attack is high then the tendency of air to turn is large.

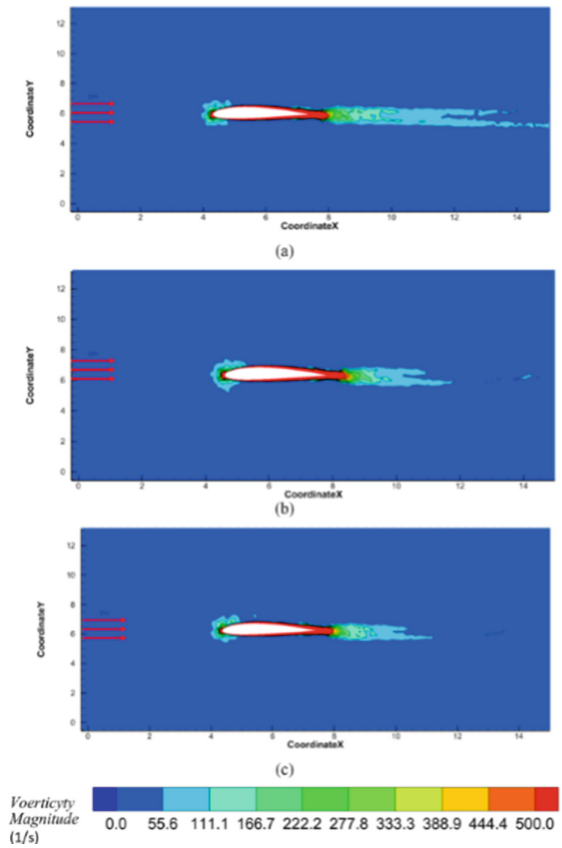


Fig. 8. Vorticity Magnitude $\alpha = 0^\circ$. (a) NACA 2412 without VG (b) NACA 2412 with 10% VG (c) NACA 2412 with 15% VG

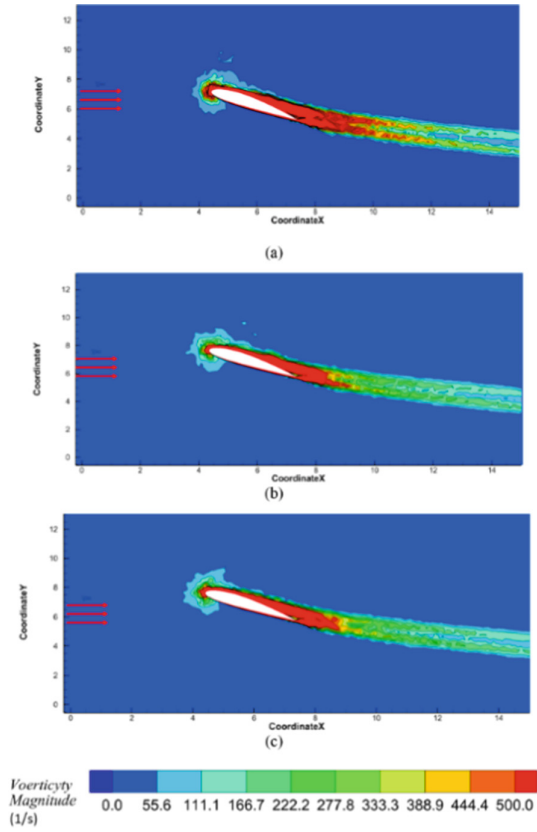


Fig. 9. Vorticity Magnitude $\alpha = 17^\circ$. (a) NACA 2412 without VG (b) NACA 2412 with 10% VG (c) NACA 2412 with 15% VG

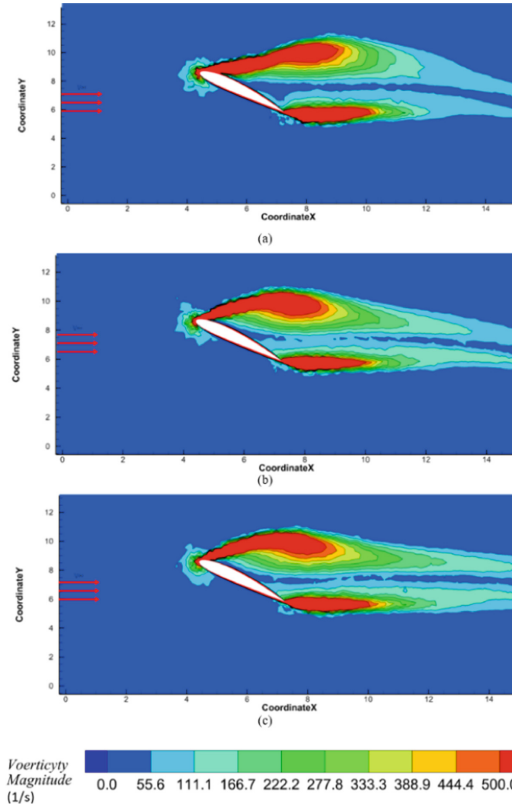


Fig. 10. Vorticity Magnitude $\alpha = 25^\circ$. (a) NACA 2412 without VG (b) NACA 2412 with 10% VG (c) NACA 2412 with 15% VG

3.6 Pressure Coefficient Contour

These pressure contours explain how the pressure spread when the air passes through the wing surface, with a variety of angles the pressure spread will be different. On the plain wing, there will be generated tip vortex at the wingtip as shown in Fig. 12. Figure 11 shows the pressure contour from NACA 2412 at $\alpha = 0^\circ$, from Fig. 11 can be seen there is decreasing pressure at area maximum thickness on airfoil Fig. 11 (a), (b), and (c) caused by there is increasing air speed on that area. There is higher pressure at the leading edge airfoil caused by decreasing air speed when passing through the leading edge airfoil. Figure 12 is a pressure contour from NACA 2412 at $\alpha = 17^\circ$, from Fig. 12, there is an area of blue color at the leading edge area that describes the lowest pressure that happened in that area, this is caused by there is high-speed air passing through the leading edge. On a plain airfoil (Fig. 12 (a)) there is an area colored yellow on the upper surface trailing edge wing describes there is increasing pressure on that area caused by

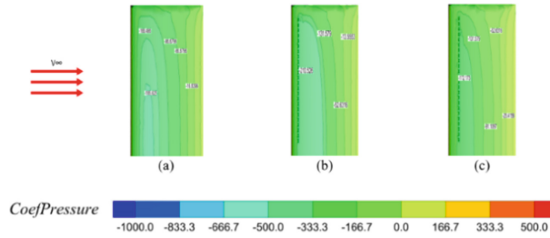


Fig. 11. Pressure coefficient contour $\alpha = 0^\circ$. (a) NACA 2412 without VG (b) NACA 2412 with 10% VG (c) NACA 2412 with 15% VG

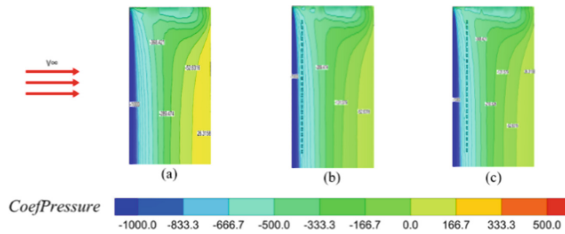


Fig. 12. Pressure coefficient contour $\alpha = 17^\circ$. (a) NACA 2412 without VG (b) NACA 2412 with 10% VG (c) NACA 2412 with 15% VG

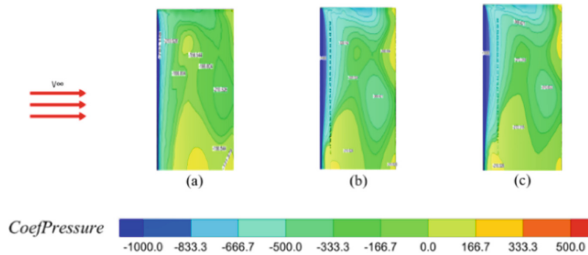


Fig. 13. Pressure coefficient contour $\alpha = 25^\circ$. (a) NACA 2412 without VG (b) NACA 2412 with 10% VG (c) NACA 2412 with 15% VG

there is flow separation so the airspeed on that area is decreasing. Figure 13 is a figure of pressure contour from NACA 2412 at $\alpha = 25^\circ$, from Fig. 13 can be seen there is random pressure spread that describes there is flow separation when passing through the wing surface and all of the wing condition is stalled.

4 Conclusion

From the explanation of the results of this study, it can be concluded several things, including:

1. With an additional gothic vortex generator on NACA 2412, the angle of attack increases can minimize the air friction with the wing surface because there is the

vortex produced by the vortex generator when the air passes through, so the airflow can be maintained from the leading edge to the trailing edge.

2. NACA 2412 without a vortex generator has flow separation earlier than the NACA 2412 with an additional vortex generator, this is caused by at the high angle of attack, the air passing through the wing surface without a vortex generator will have friction on the wing surface so the airspeed will decrease and creating the difference between the air pressure near the surface of the wing and the atmospheric pressure so the flow separation will be produced.
3. At the $\alpha = 15^\circ$, the wing without a vortex generator has airflow separation. While on the wing with an additional vortex generator, airflow separation is produced at $\alpha = 19^\circ$ which can be concluded that the additional vortex generator can be delaying the air flow separation when passing through the wing surface.
4. From the tabulation and visualization of the simulation result, can be concluded that NACA 2412 additional vortex generator at 15% installation position from leading edge direct to chord line is the most effective than the vortex generator at 10% installation position from leading edge direct to chord line.

References

1. O. López Calle, Preliminary study of the effects of vortex generators in ultralight aircraft, (2015) 71.
2. A. Boonloi, W. Jedsadaratanachai, Numerical investigations on heat transfer and flow structure in a circular tube with various shapes of winglet vortex generators, *Front. Heat Mass Transf.* 7 (2016). <https://doi.org/10.5098/hmt.7.22>.
3. C.M. Velte, M.O.L. Hansen, V.L. Okulov, Multiple vortex structures in the wake of a rectangular winglet in ground effect, *Exp. Therm. Fluid Sci.* 72 (2016) 31–39. <https://doi.org/https://doi.org/10.1016/j.expthermflusci.2015.10.026>.
4. H. Shim, J. Lee, H. Chae, S.-O. Park, Wake Characteristics of Vane-Type Vortex Generator, *Proc. 2nd World Congr. Momentum, Heat Mass Transf.* (2017) 1–8. <https://doi.org/10.11159/enfht17.102>.
5. N. Mulvany, L. Chen, J. Tu, B. Anderson, Steady-State Evaluation of Two-Equation RANS (Reynolds-Averaged Navier-Stokes) Turbulence Models for High-Reynolds Number Hydrodynamic Flow Simulations, *Dep. Defence, Aust. Gov.* (2004) 1–54.
6. S.P.S. Hariyadi, B. Junipitoyo, Sutardi, W.A. Widodo, Stall Behavior Curved Planform Wing Analysis with Low Reynolds Number on Aerodynamic Performances of Wing Airfoil Eppler 562, *J. Mech. Eng.* 19 (2022) 201–220.
7. J.D. Anderson, *Fundamentals of Aerodynamics* (6th edition), McGraw-Hill, 2011.
8. S.G. Kontogiannis, D.E. Mazarakos, V. Kostopoulos, ATLAS IV wing aerodynamic design: From conceptual approach to detailed optimization, *Aerosp. Sci. Technol.* 56 (2016) 135–147. <https://doi.org/https://doi.org/10.1016/j.ast.2016.07.002>.

Open Access This chapter is licensed under the terms of the Creative Commons Attribution-NonCommercial 4.0 International License (<http://creativecommons.org/licenses/by-nc/4.0/>), which permits any noncommercial use, sharing, adaptation, distribution and reproduction in any medium or format, as long as you give appropriate credit to the original author(s) and the source, provide a link to the Creative Commons license and indicate if changes were made.

The images or other third party material in this chapter are included in the chapter's Creative Commons license, unless indicated otherwise in a credit line to the material. If material is not included in the chapter's Creative Commons license and your intended use is not permitted by statutory regulation or exceeds the permitted use, you will need to obtain permission directly from the copyright holder.

